Uptake of Acetic Acid on Thin Ammonium Nitrate Films as a Function of Temperature and Relative Humidity

John E. Shilling and Margaret A. Tolbert*

CIRES and Department of Chemistry and Biochemistry, University of Colorado, Boulder, Colorado 80309-0216

Received: August 26, 2004; In Final Form: October 6, 2004

The interaction of acetic acid with thin ammonium nitrate (AN) films has been studied using a Knudsen cell-flow reactor coupled with Fourier transform infrared−reflection absorption spectroscopy (FTIR−RAS). The gas phase was monitored with a quadrupole mass spectrometer (MS). The combination of mass spectrometry and FTIR−RAS allows for the simultaneous observation of the gas and condensed phases, respectively. Initial uptake coefficients (γ values) and coverages (θ values) were determined from MS data over the temperature range of 200−240 K. The initial uptake coefficient varied from $\gamma = 0.058$ to 0.0024 for temperatures from 200 to 240 K, respectively, and was independent of pressure over the range 5.7×10^{-8} to 5.1×10^{-6} Torr. The temperature-dependent uptake coefficients were analyzed using a precursor-mediated adsorption model to determine $\Delta H_{obs} = -32.3$ kJ mol^{-1} and $\Delta S_{obs} = -182.2$ J K^{-1} mol^{-1}. In the absence of water vapor [relative humidity (RH) < 1%], integrated coverages for acetic acid on ammonium nitrate ranged from $\theta = 19.6$ monolayers (MLs) (9.4×10^{15} molecules cm^{-2}) at 200 K to $\theta = 0.40$ ML (2.1×10^{14} molecules cm^{-2}) at 240 K. The uptake was largely irreversible, with ∼15% of the adsorbed molecules isothermally desorbing from the film. The IR spectra revealed that acetic acid ionized on the surface, despite the fact that the ammonium nitrate film was effloresced. Adding small amounts of water vapor (4% RH) to the chamber resulted in unsaturated uptake and dramatically increased values of θ and γ. Higher RH resulted in further increases of both θ and γ. The IR spectra again revealed that acetic acid ionized on the surface. Furthermore, the formation of a liquid layer was observed in the infrared when the acetic acid was taken up by the film at RH > 10%. This observation suggests that the adsorption of water-soluble organics onto inorganic aerosol may dramatically enhance the ability of the aerosol to take up water at low RH.

Introduction

It is now well-recognized that tropospheric particles consist of a complex mixture of inorganic and organic components.[1] Therefore, it is important to understand how organic compounds interact with inorganic salt aerosol. To this end, many studies have investigated the effect of organics on the water-uptake properties of inorganic aerosol particles.[2−9] The water-uptake properties of the aerosol determine the aerosol phase and size, important properties for predicting the effects of aerosol on human health, visibility, climate forcing, and chemical reactivity.

While sulfate aerosol is thought to be the predominant inorganic component of the global tropospheric aerosol, ammonium nitrate (AN) can also be important regionally. AN composes a large fraction of the aerosol in areas where agricultural NH_3 emissions mix with air containing HNO_3. Southern California and Denver, Colorado, are major population centers that are particularly affected by AN pollution.[10−15] AN particles are estimated to be responsible for 40% of the light scattering in the Los Angeles Basin[16] and 17% of the light scattering in Denver.[17] Groblicki et al. estimate that the light scattering by the aerosol in Denver would decline by 38% if all of the water were removed from it.[17] Clearly, the water content of aerosol particles is an important determinant in an aerosol's effect on visibility.

The water content of an inorganic aerosol is dependent on both the relative humidity (RH) and its physical state. Crystalline salts exposed to increasing RH do not take up water until their characteristic deliquescence relative humidity (DRH). Once the aerosol has deliquesced, it remains an aqueous solution until the RH falls below the efflorescence relative humidity (ERH) of the salt, which is lower than its DRH. The DRH of pure AN has been determined to be 62% RH at 298 K.[9] Determination of the effloresce relative humidity has been more problematic; researchers report that AN remains an anhydrous liquid down to ∼0% RH.[9,18] For this reason, AN is often assumed to be present in the atmosphere as a liquid; however, a recent study suggests that the presence of solid inclusions or multiple inorganic components induce crystalization to solid AN.[19]

Acetic acid (HAc) is one of most common organic acids found in the troposphere. While the concentration of gas-phase HAc depends strongly on the location, it has been identified at significant levels in both polluted and pristine environments.[20] Levels of HAc over rural midlatitude forested regions have been measured to be 1.3−2.1 parts per billion by volume (ppbv) during the growing season near ground level.[21,22] The concentration of HAc was observed to be 140 ppbv higher in forest fire smoke plumes than background levels.[23] While HAc mixing ratios are generally higher in the boundary layer than in the free troposphere, significant amounts of HAc are present at higher altitudes.[24] Over the South Atlantic Basin, Jacob et al. report HAc mixing ratios of 2.6 ppbv at an altitude of 4−8 km and 1.9 ppbv at 8−12 km.[25]

Although many studies have investigated the water-uptake properties of mixed organic/inorganic aerosols, there are

* To whom correspondence should be addressed. E-mail tolbert@colorado.edu.

10.1021/jp046135z CCC: $27.50
Published on Web 11/25/2004

relatively few studies measuring the uptake of organic compounds onto model aerosol particles.[26−31] To investigate possible interactions of HAc with tropospheric surfaces, we have measured the uptake of HAc on AN using a Knudsen cell-flow reactor[32] coupled with Fourier transform infrared−reflection absorption spectroscopy (FTIR−RAS).[33] The combination of these two techniques allows us to simultaneously monitor both the gas and condensed phases. Experiments were conducted over the temperature range of 200−240 K and as a function of the HAc pressure and RH at 210 K. Our results show that the uptake of HAc on AN is efficient under a wide range of upper tropospheric conditions. This reaction represents a previously unidentified sink for gas-phase HAc. Furthermore, we show that the uptake of HAc dramatically alters the water-uptake properties of the AN film, which could affect the growth and optical properties of the aerosol.

Experimental Procedure

Vacuum Chamber. Experiments were conduced in a high-vacuum stainless-steel Knudsen flow chamber equipped with FTIR−RAS. This instrument has been previously described in detail.[28] Briefly, the infrared beam from a Nicolet Magna 550 spectrometer passes into the vacuum chamber where it is reflected from a gold substrate ($d = 2.54$ cm) at a grazing angle of 87° from the surface normal. The beam exits the chamber and is detected with a mercury/cadmium telluride (MCT-A) detector. The temperature of the substrate is controlled by resistively heating against a differentially pumped liquid-nitrogen cryostat. Temperature is monitored with a T-type thermocouple attached directly to the substrate. The thermocouple is calibrated with respect to the ice frost point.[34] A Teflon seal surrounds the substrate and separates the chamber from the cryostat, ensuring that the gold is the only cold surface exposed to the chamber atmosphere. A Teflon cup, mounted on a pneumatic linear translator, allows the surface to be isolated from or exposed to the chamber atmosphere without significantly altering the chamber volume. Three leak valves are used to introduce the gas-phase species of interest into the chamber, and pressure is monitored using a Baratron capacitance manometer (Baratron 690A) and an ionization gauge. RH is determined by taking the ratio of the measured water partial pressure to the vapor pressure of water, as determined from the Wexler expression, at the substrate temperature.[35] HAc and water vapor are drawn from bulbs containing glacial HAc (ACS grade) and water (HPLC grade), respectively, that have been subjected to several freeze−pump−thaw cycles. Nitric acid vapor was drawn from a bulb containing a mixture of 3:1 H_2SO_4(ACS grade)/HNO_3(ACS grade) that had also been degassed by several freeze−pump−thaw cycles. Ammonia (anhydrous grade) was drawn directly from a gas cylinder and used without further purification. Trace gas-phase species are monitored using a MS (UTI 100C), which is calibrated to the ionization gauge and the Baratron. Using this procedure, the absolute pressure of the trace gases can be obtained with the MS. The condensed phase is simultaneously monitored using FTIR−RAS when the Teflon cup is open. In experiments where no water was added to the chamber, the total pressure was equal to the HAc partial pressure or the background pressure of $\sim 1 \times 10^{-6}$, whichever is higher. In experiments where water was added to the chamber, the total pressure was equal to the water partial pressure. In all cases, the total pressure was below that required to operate the Knudsen cell in the molecular flow regime.

AN Film Preparation. Thin films of AN are prepared by vapor deposition as illustrated in Figure 1. The spectra in this figure have been offset for clarity. First, HNO_3 is deposited on the substrate at 160 K to a thickness of ~30 nm (spectrum A). This film is then exposed to a high partial pressure (5×10^{-3} Torr) of gas-phase NH_3 (spectrum B). The NH_3 is then pumped off, and the film is annealed to 260 K to remove any unreacted HNO_3 and to crystallize the film. A spectrum of the resultant NH_4NO_3 film is shown in C and agrees well with literature spectra of crystalline AN.[36] The lack of scattering at the high-energy end of the spectrum indicates that the film is flat, at least on the scale of $\lambda/10$ (~200 nm). We believe that the film is fully effloresced at this point; there are no liquid-water features present in the IR spectra. Furthermore, we see no evidence of liquid-water uptake in the IR if the sample is exposed to increasing amounts of water vapor. Water uptake on the pure AN film and the HAc-doped film will be discussed in more detail later in this paper.

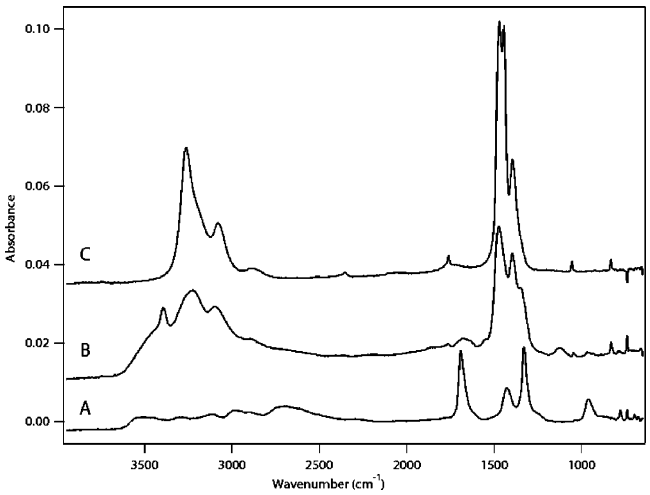

Figure 1. IR spectra detailing the preparation of thin AN films. The spectra have been offset for clarity. Spectrum A shows the deposition of HNO_3 at 160 K. Spectrum B shows the film at 160 K after the addition of gas-phase NH_3. Spectrum C shows the resultant AN film after annealing to 260 K.

General Procedure. Once the sample has been prepared, the Teflon cup is extended to isolate the substrate from the chamber atmosphere. HAc is admitted into the chamber and monitored at $m/z = 60.0$ with the MS. The flow of HAc is adjusted until the signal reaches the desired level and is stable. For the experiments described herein, this flow corresponds to an HAc partial pressure from 5.7×10^{-8} to 5.1×10^{-6} Torr. It is known that carboxylic acids dimerize in the gas phase. A value of $K_{eq} = [\text{dimer}]/[\text{monomer}]^2 = 2.5$ Torr^{-1} has been reported for HAc at 295 K.[37] Gas-phase HAc will quickly equilibrate with the reactor walls, which are at room temperature; therefore, this value of K_{eq} accurately represents our experimental conditions. Using this value of K_{eq}, we find that the dimer concentration is a factor of $\sim 10^5$ smaller than the monomer concentration under the highest pressures of HAc studied herein. Therefore, the presence of the gas-phase HAc dimer has been ignored in our data analysis.

When the flow is stable, the cup is retracted, exposing the sample to the gas-phase HAc. If uptake occurs, a decrease in the MS signal is observed. Using the Knudsen effusion relation, the initial uptake coefficient (γ) can be calculated according to eq 1 where S_0 is the initial MS signal, S is the signal after the

$$\gamma = \frac{A_h(S_0 - S)}{A_s S} \tag{1}$$

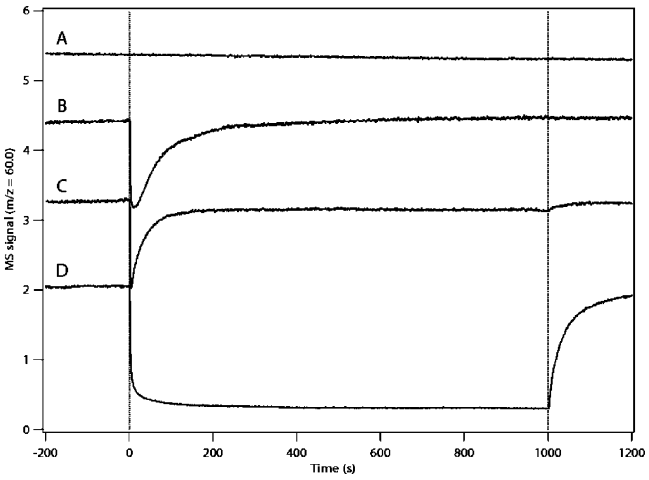

Figure 2. Raw mass spectral data obtained at $m/z = 60.0$ for HAc adsorption onto the substrate. Trace A shows the signal during a control experiment on the blank gold substrate. Traces B and C show the uptake onto AN films in the absence of additional water vapor at 210 and 200 K, respectively. Trace C shows the uptake onto an AN film at 210 K and 37% RH. Vertical lines have been drawn at $t = 0$ and 1000 s to show when the substrate was exposed to and isolated from the gas-phase HAc. For clarity, trace A has been offset by 3.5 units, trace B has been offset by 2.25 units, and trace C has been offset by 1.0 unit.

cup is opened, A_h is the area of the escape orifice (0.19 cm^2), and A_S is the surface area of the sample.[38] In all calculations, the geometric surface area of the gold substrate (5.07 cm^2) was used to approximate the surface area of the sample. We believe that this approximation is valid for several reasons. First, FTIR−RAS is very sensitive to light scattering; therefore, the lack of scatter in the IR spectra indicates that the deposited film is smooth on the length scales of IR light.[39] Second, the AN films have a low vapor pressure and were grown at very low temperatures, conditions that lend themselves to the growth of smooth films. With the current apparatus, we can measure values of γ between 0.001 and 0.3.

The integrated area under the uptake curve is used to calculate the number of molecules lost to the surface, which is divided by the surface area of the substrate to yield the surface coverage (θ). The coverage limit of detection is approximately 0.1 monolayer (ML). If a sufficient surface coverage is reached, condensed phase products can be identified in the IR. After 1000 s of exposure time, the cup is closed and the signal is allowed to recover to its original level. The flow of HAc is then turned off, and the chamber is evacuated. The cup is then opened again, and HAc is allowed to isothermally desorb. The area of this desorption peak can then be compared with the area of the adsorption peak to make an estimate of the percentage of molecules that isothermally desorb from the film.

Results and Discussion

Figure 2 shows typical raw experimental data for the uptake of HAc on AN under a variety of experimental conditions. Trace A shows the HAc signal for exposure to the blank gold substrate at 200 K. Traces B and C were recorded in the absence of additional water vapor at 210 and 200 K, respectively. Trace D was recorded at 210 K and 37% RH. For clarity, trace A has been offset by 3.5 units, trace B has been offset by 2.25 units, and trace C has been offset by 1.0 unit. All experiments were conducted at the same nominal HAc pressure. At the pressures used in this study, there is no adsorption of HAc onto the blank gold substrate (trace A). As seen in this figure, three distinctly different uptake regimes were observed, saturated (trace B), unsaturated uptake with partial recovery of the signal (trace C), and unsaturated uptake with no recovery of the signal (trace D). Saturated uptake (trace B) is marked by a slow recovery of the HAc signal to its original value after the initial uptake. When the cup is closed at $t = 1000$ s, there is no change in the MS signal, indicating that the surface has fully saturated at this point. After saturation, the coverage of HAc on AN is independent of the total dose of acid. Saturated uptake was observed in the absence of water vapor at $T > 200$ K.

The second type of uptake behavior observed in this study is illustrated in trace C. In this uptake regime, the signal drops when the cup is opened and recovers, as in trace B. However, the signal reaches a steady state at a level that is slightly below its original level. At this point, the AN film is continuously taking up a very small amount of HAc. As a result, the coverage is dependent on the dose of HAc. When the cup is closed at $t = 1000$ s, the signal fully recovers to its original level. This type of behavior was consistently observed at $T = 200$ K and in two of the seven experiments at 210 K, in the absence of water vapor.

The aforementioned uptake behaviors are in contrast with the MS signal observed in the uptake regime shown in trace D. Here, the signal shows no sign of recovery after 1000 s. When the cup is closed, the signal begins to recover to its original value. The coverage of HAc on AN in this regime is determined to a large extent by the length of time that the cup is opened. Longer exposure times lead to larger coverages. We will present evidence later in this paper showing that the uptake in the unsaturated regimes are not simply condensation of molecular HAc onto the substrate.

Figure 3 shows the initial uptake coefficients (A) and coverages (B) obtained for the uptake of HAc onto crystalline AN as a function of the temperature at RH < 1%. No water vapor was admitted to the chamber during these experiments. All points on the graph are an average value of at least six separate experiments conducted at that temperature. Error bars are determined by performing a *t* test at the 95% confidence limit on the data. The coverages shown in B have been converted into ML units by dividing the observed uptake by the ML coverage of HAc (4.8×10^{14} molecules cm^{-2}). The ML coverage was calculated from the bulk density of HAc (1.049 g/cm^3) and is therefore approximate. The experiments shown in Figure 3 were performed at an HAc partial pressure ranging from 2.5 to 4.6×10^{-6} Torr. As can be seen in Figure 3, both the coverage and the uptake coefficients increase dramatically as the temperature is decreased. The values of the uptake coefficient range from $\gamma = 0.058$ at 200 K to $\gamma = 0.0024$ at 240 K. For comparison the uptake coefficient for HAc on pure water at 273 K is 0.067.[27] Clearly, the uptake of HAc onto effloresced AN is quite efficient. Note that we are reporting initial uptake coefficients, not mass accommodation coefficients. As such, the desorption of molecules from the solid phase is not taken into account. Therefore, the values of γ reported in this work may be lower limits to the mass accommodation coefficient under similar conditions. However, a recent model by Ammann et al. suggests that desporption effects are negligible when the surface coverage is much less than one ML.[40] Indeed, all of the values of γ reported herein were calculated when the coverage of HAc on the surface was much less than one ML.

To ensure that the uptake coefficients reported here are accurate under tropospheric conditions, we have measured γ under a range of HAc partial pressures. The results of the individual experiments conducted at 210 K are shown in Figure 4. Over the range of pressures studied, from 5.7×10^{-8} to 5.1

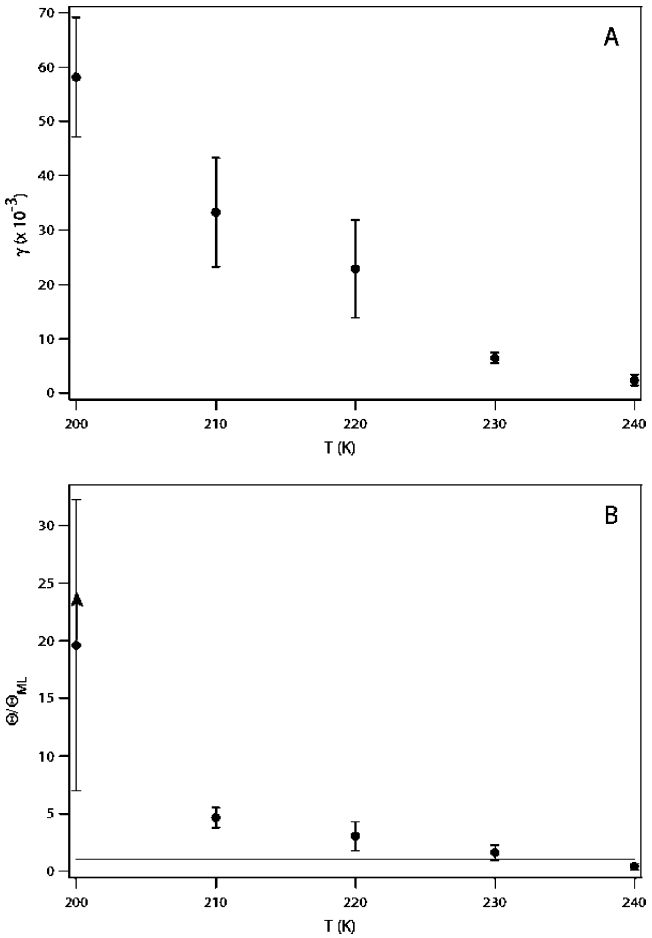

Figure 3. Data obtained for the uptake of HAc on AN as a function of the temperature. (A) Initial uptake coefficients. (B) Ratio of the observed coverage to the calculated ML coverage. The line in plot B indicates 1 ML. The arrow on the data point at 200 K indicates that the coverage did not saturate on the time scale of the experiment (1000 s).

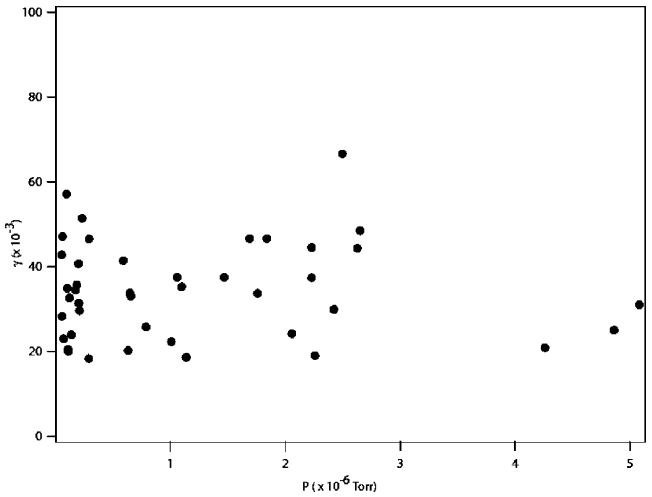

Figure 4. Initial uptake coefficients for HAc adsorption onto dry AN films at 210 K as a function of HAc pressure.

$\times 10^{-6}$ Torr, the initial uptake coefficients are independent of the partial pressure, within error. Measurements of tropospheric HAc levels generally fall within this pressure range.

The coverages of HAc on AN are also large, ranging from 20 to 0.5 ML from 200 to 240 K, respectively. The uptake at 200 K did not saturate on the time scale of the experiment (1000 s); the signal reached a steady-state value below the level of the original signal and showed no signs of further recovery, as seen in trace C of Figure 2. The steady-state uptake coefficient at this point is $\gamma \sim 2 \times 10^{-3}$, which is small when compared to the initial uptake coefficient but above the detection limit. Later in this paper, we show that the uptake of HAc onto AN is extremely sensitive to the chamber RH. In light of this, we believe that small amounts of residual water outgassing from the chamber walls and gas handling lines are raising the RH past the threshold value necessary for unsaturated uptake. MS scans of the background gases in our chamber prior to the start of experiments consistently reveal that the majority of the background gas is water vapor. In fact, the water vapor signal is generally 5 times greater than the next largest signal (N_2). In a few select experiments at 200 K and RH < 1%, the background water signal was monitored with the MS. In these experiments, uptake of background water onto the AN film was observed. Although we do not have an accurate measure of the RH at this point, we can set an upper limit of RH < 1%. The data point at 200 K represents the amount of HAc adsorbed after 1000 s of exposure; therefore, it is a lower limit on what the saturated coverage would be at this temperature. In an attempt to identify any gas-phase products that are released, mass scans were taken while uptake was occurring. During these experiments, no gas-phase products were detected. We specifically looked for the evolution of water and nitric acid during a few select experiments, but neither of these compounds was detected in the gas phase. However, condensed-phase products were observed in the IR spectra.

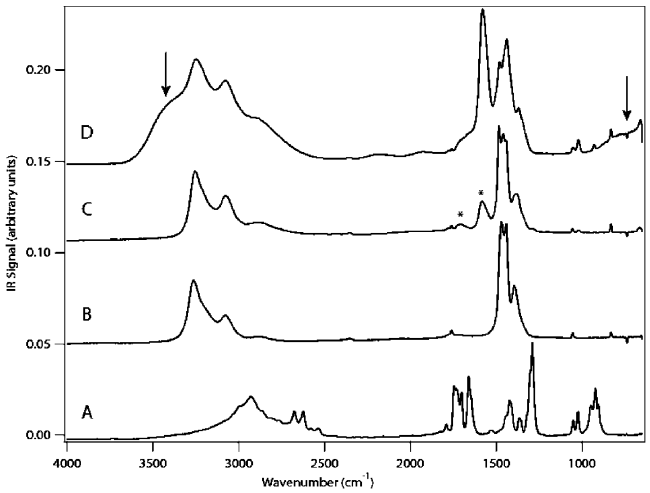

Figure 5. IR spectra of the species studied in this work. Spectrum A is solid HAc at 160 K. Spectrum B is AN at 200 K. Spectrum C shows the AN film after exposure to HAc at 200 K. Peaks attributed to the formation of the CH_3COO^- ion are highlighted with an asterisk. Spectrum D shows the AN film after exposure to HAc at 210 K and 37% RH. Liquid-water peaks have been indicated with an arrow. The spectra have been offset for clarity and are not on a common scale.

Figure 5 shows IR spectra of the condensed-phase products of HAc on AN obtained under a variety of conditions; the spectra have been offset for clarity and are not all on a common scale. Spectra A and B are solid HAc and AN, respectively, and are shown for reference. Spectrum C shows the AN at 200 K after approximately 1000 s of exposure to HAc at RH < 1%. When this spectrum is compared to that of condensed HAc, one can clearly see that molecular HAc is not simply condensing on the AN at 200 K. An experiment at 200 K was conducted in which the HAc partial pressure was incrementally increased up to a factor of 8−10 times higher than the pressures used in this study. During this experiment, no condensation of HAc was observed with the IR. Furthermore, the vapor pressure of solid

HAc at 200 K reported in the literature is 2.8×10^{-5} Torr, which is well above the partial pressure of HAc used in these studies ($2.5-4.6 \times 10^{-6}$ Torr).[41] Finally, experiments in which HAc was exposed to the bare gold surface at 200 K (trace A of Figure 2) showed no uptake. Instead, the most obvious spectral change is the feature growing in at 1580 cm^{-1}. We have assigned this peak as the C−O stretch of the acetate-ion-based literature spectra of sodium acetate [42,43] and of HAc ionizing on surfaces.[44,45] This peak is absent in the spectrum of molecular HAc shown in spectrum A and in the literature spectra of unionized HAc.[42,43] A less intense peak at 1708 cm^{-1} is also observed to grow into the IR spectrum. The assignment of this peak is more tenuous. We attribute this peak to the bending mode of the H_3O^+ ion, on the basis of the intensity of the peak and literature spectra.[46] There is no peak at this location in the spectra of the acetate ion.[42,43] However, the C═O stretch of molecular HAc does absorb here.[42,43,45] It is possible that a small amount of HAc physisorbs and remains unionized on the surface. We do not see a loss of AN in the infrared, and no gas-phase products were detected with the MS. In light of these observations, we believe that ionization, as shown in eq 2 is

$$CH_3COOH\ (g) + H_2O\ (ad) \rightarrow CH_3COO^-\ (ad) + H_3O^+\ (ad) \quad (2)$$

the only chemical reaction occurring when HAc adsorbs on AN. Although we believe that the HAc is ionized upon uptake, we also believe that the film is fully effloresced under these experimental conditions. Therefore, we hypothesize that a limited amount of surface-adsorbed water controls the ionization. Once this limited amount of water is consumed by the ionization, the uptake is no longer thermodynamically favorable and halts.

To elucidate the importance of water on the uptake of HAc on AN, a series of experiments were conducted in which the temperature was held constant at 210 K and the RH was varied. Figure 6 shows the effect of increasing RH on the initial uptake coefficients (A) and coverages (B). For the substrate temperature of 210 K, the data points at 0, 4.4, 10.0, 18.6, and 37.4% RH correspond to water partial pressures of $<10^{-6}$, 4.4×10^{-4}, 1.0×10^{-3}, 1.9×10^{-3}, and 4.4×10^{-3} Torr, respectively. As can be seen, the uptake coefficients increase dramatically with RH, ranging from $\gamma = 0.03$ at <1% RH to $\gamma = 0.24$ at 37% RH. Higher RH always resulted in an increase in γ. At 37% RH, we are near our upper limit of detection; the signal essentially drops to the background level of HAc upon opening the cup. The addition of water vapor to the chamber also had a dramatic effect on the observed coverages. The addition of a small amount of water vapor (4% RH) shifted the uptake regime from saturated to unsaturated. As a result, all of the coverages shown in Figure 6 at RH >1% are lower limits of the maximum uptake under those conditions. The coverage at 4% RH is a factor of 7 larger than the coverage at RH < 1%. Further addition of water vapor resulted in further increases in the coverage, until it begins to plateau around 20% RH. At this point, the coverage is limited only by the flow of acid into the chamber and the integration time; essentially, all of the HAc admitted to the chamber is taken up by the film. These results show that the RH is even more important than the temperature in controlling the uptake of HAc on AN.

The infrared spectrum of the products in the presence of 37% RH is shown in spectrum D of Figure 5. In addition to the peaks growing into the spectrum at 1580 and 1708 cm^{-1}, there are now clearly changes around 3400 and 700 cm^{-1}. These features are attributed to the OH stretch and libration, respectively, of

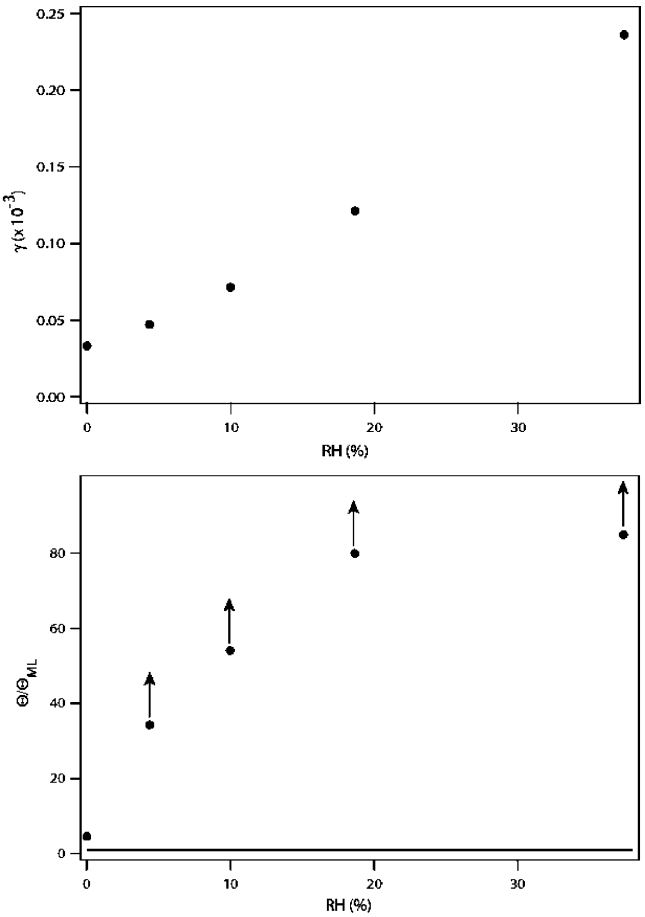

Figure 6. Data obtained for the uptake of HAc on AN at 210 K as a function of the RH. (A) Initial uptake coefficients. (B) Ratio of the observed coverage to the calculated ML coverage. The line in B indicates 1 ML. The arrows on the data points at RH > 1% indicate that the coverage did not saturate on the time scale of the experiments (1000 s).

liquid water. Liquid-water features were clearly observed in the condensed-phase spectra when HAc adsorbed onto AN at RH > 10%. These features continued to grow into the IR with HAc exposure, indicating that water and HAc are simultaneously adsorbed to the film. Liquid-water features were not observed in the AN spectrum at theses relative humidities in the absence of HAc.

It is unclear from the spectrum whether the film is fully deliquesced or is made up of a liquid layer rich in HAc, AN, and water over solid AN. However, it is clear that the adsorption of HAc is altering the water-uptake properties of AN at RHs that are quite low. Interestingly, films containing this liquid water were clearly visible with the naked eye, while the dry films were not. Thus, the presence of HAc and water vapor together affected the growth and optical properties of the AN film. Unfortunately, we are not able to quantify the water uptake; therefore, we are unable to report growth curves for this system. However, we can estimate the mass of HAc and AN present in the film and set a lower bound on the water content of the film. The mass of HNO_3 deposited in the initial stages of the AN film preparation can be calculated directly from Baratron pressure data. Assuming that all of the deposited HNO_3 is neutralized, we can estimate the mass of the AN film. As described previously, the integrated area under the uptake curve yields the mass of HAc that is taken up by the film. Assuming that at least one water molecule is necessary to ionize one HAc molecule, we can set the lower bound on the water content of

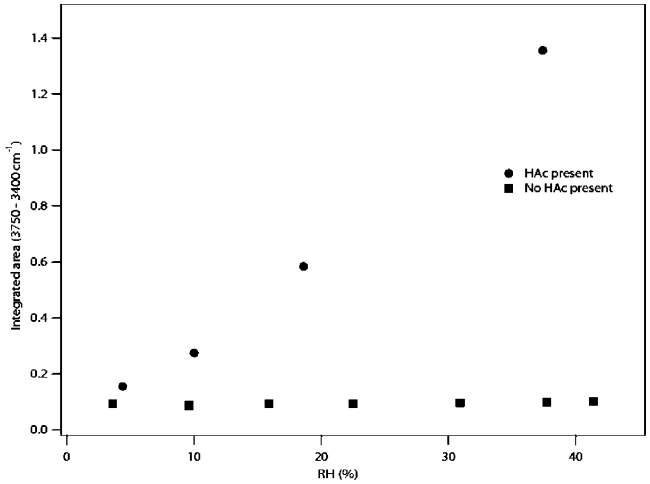

Figure 7. Integrated area of the liquid-water OH stretch from 3750 to 3400 cm^{-1} as a function of the RH. The circles represent this area in the presence of HAc, and the squares represent this area in the absence of HAc.

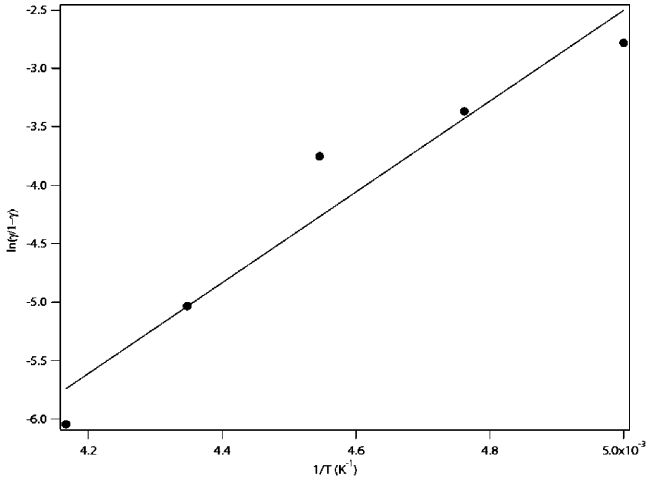

Figure 8. Fit of the temperature-dependent γ data according to eq 4. Values of $\Delta H_{obs} = -32.3$ kJ mol^{-1} and $\Delta S_{obs} = -182.2$ J K^{-1} mol^{-1} were extracted from the slope and intercept, respectively.

the film. Using these assumptions, we estimate that the composition of the films shown in spectrum D of Figure 5 is 55% AN, 34% HAc, and 11% water by mass. Using the same numbers, we estimate that the volume of the film has increased by a minimum of 81% because of the adsorption of water and HAc. Again, these estimates represent a lower bound for the amount of water adsorbed; the actual amount and thus the growth factor is likely to be significantly larger.

To better illustrate the effect of acetic acid on the liquid-water content of the AN film, the integrated area of the liquid-water OH-stretching region from 3750 to 3400 cm^{-1} has been plotted as a function of RH in Figure 7 for two films at 210 K. As indicated by the squares in this figure, there are no changes in the liquid-water region of the infrared in the absence of HAc as the RH is increased. This is not surprising, considering a crystalline salt is not predicted to take up water until its characteristic DRH. The DRH of AN at 298 K has been measured to be 62%.[9] Although the DRH at 210 K is unknown, a thermodynamic model predicts that the DRH for AN is 85% RH at the eutectic temperature of 256.8 K.[47] The same model predicts that the DRH of AN is inversely related to the temperature; therefore, the DRH at 210 K should be greater than the DRH at the eutectic temperature.[47] In contrast, the area of the liquid-water peak is strongly dependent on the RH in the presence of HAc. From this figure, we can conclude that the adsorption of HAc onto AN enhances its water content at RHs as low as 10%.

After each uptake experiment, the area of the isothermal desorption peak was measured, as previously described. Comparing the number of molecules that isothermally desorb to the number of molecules that adsorbed gives an estimate of the reversibility of the adsorption process. When no water vapor was added to the chamber, approximately 15% of the molecules that adsorb on the surface isothermally desorb. This percentage is independent of the temperature. The low percentage of molecules that isothermally desorb from the film suggests that the uptake is largely irreversible at all of the temperatures studied in this work. The desorption process was more complicated in the experiments involving RH > 1%. In these experiments, both the water and HAc flows were turned off before the desorption peak was measured. Here, the desorption percentage varied exponentially with the initial RH, with 53% desorption at 4% RH and 3% desorption at 37% RH. The water incorporated in the film appears to help the AN retain adsorbed HAc.

To get a more quantitative understanding of the adsorption process, the uptake coefficients of HAc on AN at RH < 1% have been analyzed using a precursor-mediated adsorption model as described in previous publications.[27,39] The overall reaction scheme is shown in eq 3 where HAc (g), HAc (p), and

$$\text{HAc (g)} \underset{k_{des}}{\overset{\alpha k_{coll}}{\rightleftharpoons}} \text{HAc (p)} \xrightarrow{k_{ads}} \text{HAc (c)} \qquad (3)$$

HAc (c) represent gas-phase, physisorbed, and chemisorbed HAc, respectively. In this model, molecules in the gas phase are in equilibrium with molecules physically adsorbed to the surface and α is assumed to be unity. Physisorbed molecules can then irreversibly chemisorb to the surface. Using this model, one can derive the relationship between γ and ΔG_{obs} shown in eq 4 From eq 4, a plot of $\ln(\gamma/(1-\gamma))$ versus $1/T$ yields a line

$$\ln\left(\frac{\gamma}{1-\gamma}\right) = -\frac{\Delta G_{obs}}{RT} = -\frac{\Delta H_{obs}}{RT} + \frac{\Delta S_{obs}}{RT} \qquad (4)$$

with slope $-\Delta H_{obs}/R$ and intercept $\Delta S_{obs}/R$. Figure 8 shows the initial uptake coefficients for HAc uptake on dry AN plotted and fit according to eq 4. From this fit, we determine $\Delta H_{obs} = -32.3$ kJ mol^{-1} and $\Delta S_{obs} = -182.2$ J K^{-1} mol^{-1}. While this value of ΔH_{obs} may seem small for chemisorption of a molecule to a surface, one must consider that the ionization is occurring on a highly ionic substrate. Bonding of ionized HAc to the AN surface would require the disruption of the lattice structure, which would be energetically unfavorable. Furthermore, the values determined here are in excellent agreement with Jayne et al., who report $\Delta H_{obs} = -33.9$ kJ mol^{-1} and $\Delta S_{obs} = -146$ J K^{-1} mol^{-1} for HAc adsorption onto pure water drops.[27] The similarity of these values lends further support to our hypothesis that surface-adsorbed water is ionizing the HAc on the AN film.

Conclusions and Atmospheric Implications

In this paper, we have shown that the adsorption of HAc onto effloresced films of AN is quite efficient at upper tropospheric temperatures. To estimate the importance of this reaction in the upper troposphere, we have calculated the lifetime of HAc in the upper troposphere under the following conditions. Neumann et al. report a fine particle mixing ratio of 1−35 ppbv,[13] which translates into a particle volume of 2−73 μm^3/cm^3. These measurements were taken under conditions where HNO_3 and fine-particle mixing ratios were anticorrelated. The authors

attribute this anticorrelation to particlulate AN formation. Assuming a particle radius of 0.4 μm yields a surface area of 16−550 $\mu m^2/cm^3$. Using our experimentally determined value of $\gamma = 0.0024$ at 240 K and RH < 1%, we obtain a lifetime for HAc between 3 and 100 h with respect to heterogeneous removal by AN, in the kinetic limit. For comparison, the lifetime of HAc with respect to the reaction with the OH radical is more than 1 week.[20] Clearly, the heterogeneous removal of HAc will dominate over gas-phase reactions, even at RH < 1%. Under atmospherically relevant RH, the lifetime of HAc would be even shorter. It should be noted that the steady-state coverage of HAc on AN at 240 K at RH < 1% is $\theta = 0.4$ ML. Therefore, if the ambient RH were less than 1%, the atmospheric loadings of AN described above could only remove a small percentage of the gas-phase HAc before becoming saturated. However, we have also shown that the presence of small amounts of water (RH = 4%) in the gas phase shifts the uptake regime from saturated to unsaturated. Therefore, under atmospherically relevant RH, AN could represent a significant sink of gas-phase HAc.

In our experiments, adding even small amounts of water vapor to the chamber (RH ~ 4%) dramatically increased the values of both θ and γ. Under conditions where RH > 10%, liquid-water features were observed to grow into the IR spectra when HAc was taken up by the film. These features were not present under similar conditions in the absence of HAc. The HAc is enhancing the water-uptake properties of the AN, allowing it to take up water at RHs well below the DRH. Therefore, AN aerosol that had been exposed to organic acids could contain liquid water under a wider range of conditions than predicted for the pure solid. The presence of a liquid layer was observed to have a dramatic effect on the growth properties of the aerosol and could affect visibility in polluted environments. Furthermore, the presence of this liquid layer could enhance heterogeneous reaction rates, because data has shown that reactions are generally faster on liquid aerosol particles.[48]

The observations presented in this paper show that volatile organics can partition into the aerosol phase. Even in the absence of water vapor, significant amounts of HAc irreversibly adsorbed onto the AN films. In the presence of water vapor, the partitioning to the film was even more dramatic. At RH > 20%, essentially all of the gas-phase HAc was taken up by the film. Clearly, even volatile organics can be present in the condensed phase at significant levels. The presence of HAc in the aerosol phase could further influence aerosol partitioning by reacting with other organics to form lower volatility products.

Acknowledgment. This work was supported by the Biological and Environmental Research Program, U.S. Department of Energy, under Grant no. DE-FG03-01ER63096 and National Science Foundation under Grant no. ATM-0137261. J.E.S. acknowledges support from the NASA ESS fellowship (NGT5-30422). J.E.S. thanks Dr. Mark Zondlo for helpful discussions concerning the data interpretation.

References and Notes

(1) Murphy, D. M.; Thomson, D. S.; Mahoney, M. J. *Science* **1998**, *282*, 1664.
(2) Brooks, S. D.; Wise, M. E.; Cushing, M.; Tolbert, M. A. *Geophys. Res. Lett.* **2002**, *29*, 23.
(3) Prenni, A. J.; DeMott, P. J.; Kreidenweis, S. M.; Sherman, D. E.; Russell, L. M.; Ming, Y. *J. Phys. Chem. A* **2001**, *105*, 11240.
(4) Wise, M. E.; Surratt, J. D.; Curtis, D. B.; Shilling, J. E.; Tolbert, M. A. *J. Geophys. Res.* **2003**, *108*, 4638.
(5) Kumar, P. P.; Broekhuizen, K.; Abbatt, J. P. D. *Atmos. Chem. Phys. Discuss.* **2003**, *3*, 949.
(6) Broekhuizen, K.; Kumar, P. P.; Abbatt, J. P. D. *Geophys. Res. Lett.* **2004**, *31*, L01107.
(7) Cruz, C. N.; Pandis, S. N. *Environ. Sci. Technol.* **2000**, *24*, 4313.
(8) Raymond, T. M.; Pandis, S. N. *J. Geophys. Res.* **2002**, *107*, 16.
(9) Lighstone, J. M.; Onasch, T. B.; Imre, D.; Oatis, S. *J. Phys. Chem. A* **2000**, *104*, 9337.
(10) Sloane, C. S.; Watson, J.; Chow, J.; Pritchett, L.; Richards, L. W. *Atmos. Environ.* **1991**, *25A*, 1013.
(11) Gordon, R. J.; Bryan, R. J. *Environ. Sci. Technol.* **1973**, *7*, 645.
(12) Solomon, P. A.; Salmon, L. G.; Fall, T.; Cass, G. R. *Environ. Sci. Technol.* **1992**, *26*, 1594.
(13) Neuman, J. A.; Nowak, J. B.; Brock, C. A.; Trainer, M.; Fehsenfeld, F. C.; Holloway, J. S.; Hubler, G.; Hudson, P. K.; Murphy, D. M.; Nicks, D. W., Jr.; Orsini, D.; Parrish, D. D.; Ryerson, T. B.; Sueper, D. T.; Sullivan, A.; Weber, R. *J. Geophys. Res.* **2003**, *108*, 4557.
(14) Russell, A. G.; McRae, G. J.; Cass, G. R. *Atmos. Environ.* **1983**, *17*, 949.
(15) Chow, J. C.; Watson, J. G.; Fujita, E. M.; Lu, Z.; Lawson, D. R.; Ashbaugh, L. L. *Atmos. Environ.* **1994**, *28*, 2061.
(16) White, W. H.; Roberts, P. T. *Atmos. Environ.* **1977**, *11*, 803.
(17) Groblicki, P. J.; Wolff, G. T.; Countess, R. J. *Atmos. Environ.* **1981**, *15*, 2473.
(18) Richardson, C. B.; Hightower, R. L. *Atmos. Environ.* **1987**, *26A*, 971.
(19) Martin, S. T.; Schlenker, J. C.; Malinowski, A.; Hung, H.-M. *Geophys. Res. Lett.* **2003**, *30*, 2102.
(20) Chebbi, A.; Carlier, P. *Atmos. Environ.* **1996**, *30*, 4233.
(21) Talbot, R. W.; Beecher, K. M.; Harriss, R. C.; Cofer, W. C., III. *J. Geophys. Res.* **1988**, *93*, 1638.
(22) Talbot, R. W.; Sosher, B. W.; Heikes, B. G.; Jacob, D. J.; Munger, J. W.; Daube, B. C.; Keene, W. C.; Maben, J. R.; Artz, R. S. *J. Geophys. Res.* **1995**, *100*, 9335.
(23) Yokelson, R. J.; Goode, J. G.; Ward, D. E.; Susott, R. A.; Babitt, R. E.; Wade, D. D.; Bertschi, I.; Griffith, D. W. T.; Hao, W. M. *J. Geophys. Res.* **1999**, *104*, 30.
(24) Talbot, R. W.; Andreae, M. O.; Berresheim, H.; Jacob, D. J.; Beecher, K. M. *J. Geophys. Res.* **1990**, *95*, 16.
(25) Jacob, D. J.; Heikes, B. G.; Fan, S.-M.; Logan, J. A.; Mauzerall, D. L.; Bradshaw, J. D.; Singh, H. B.; Gregory, G. L.; Talbot, R. W.; Blake, D. R.; Sachse, G. W. *J. Geophys. Res.* **1996**, *101*, 24235.
(26) Carlos-Cuellar, S.; Li, P.; Christensen, A. P.; Krueger, B. J.; Burrichter, C.; Grassian, V. H. *J. Phys. Chem. A* **2003**, *107*, 4250.
(27) Jayne, J. T.; Duan, S. X.; Davidovits, P.; Worsnop, D. R.; Zahniser, M. S.; Kolb, C. E. *J. Phys. Chem.* **1991**, *95*, 6329.
(28) Hudson, P. K.; Zondlo, M. A.; Tolbert, M. A. *J. Phys. Chem. A* **2002**, *106*, 2882.
(29) Sokolov, O.; Abbatt, J. P. D. *J. Phys. Chem. A* **2002**, *106*, 775.
(30) Zhang, H. Z.; Li, Y. Q.; Davidovits, P.; Williams, L. R.; Jayne, J. T.; Kolb, C. E.; Worsnop, D. R. *J. Phys. Chem. A* **2003**, *107*, 6398.
(31) Zhang, H. Z.; Li, Y. Q.; Xia, J. R.; Davidovits, P.; Williams, L. R.; Jayne, J. T.; Kolb, C. E.; Worsnop, D. R. *J. Phys. Chem. A* **2003**, *107*, 6388.
(32) Golden, D. M.; Spokes, G. N.; Benson, S. W. *Angew. Chem., Int. Ed.* **1973**, *12*, 534.
(33) Greenler, R. G. *J. Chem. Phys.* **1966**, *44*, 310.
(34) Marti, J.; Mauersberger, K. *Geophys. Res. Lett.* **1993**, *20*, 363.
(35) Wexler, A. *J. Res. Natl. Bur. Stand.* **1976**, *73A*, 493.
(36) Koch, T. G.; Holmes, N. S.; Roddis, T. B.; Sodeau, J. R. *J. Chem. Soc., Faraday Trans.* **1996**, *92*, 4787.
(37) Crawford, M. A.; Wallington, T. J.; Szente, J. J.; Maricq, M. M.; Francisco, J. S. *J. Phys. Chem. A* **1999**, *103*, 365.
(38) Barone, S. B.; Zondlo, M. A.; Tolbert, M. A. *J. Phys. Chem. A* **1997**, *101*, 8643.
(39) Hudson, P. K.; Shilling, J. E.; Tolbert, M. A.; Toon, O. B. *J. Phys. Chem. A* **2002**, *106*, 9874.
(40) Ammann, M.; Poschl, U.; Rudich, Y. *Phys. Chem. Chem. Phys.* **2003**, *5*, 351.
(41) Ambrose, D. *J. Chem. Thermodyn.* **1979**, *11*, 183.
(42) Max, J.-J.; Chapados, C. *J. Phys. Chem. A* **2004**, *108*, 3324.
(43) Quiles, F.; Burneau, A. *Vib. Spectrosc.* **1998**, *16*, 105.
(44) Jackson, S. D.; Kelley, G. J.; Lennon, D. *React. Kinet. Catal. Lett.* **2000**, *70*, 207.
(45) Tanaka, H.; Watanabe, T.; Chikazawa, M. *J. Chem. Soc., Faraday Trans.* **1997**, *93*, 4377.
(46) Zondlo, M. A.; Barone, S. B.; Tolbert, M. A. *J. Phys. Chem. A* **1998**, *102*, 5735.
(47) Tabazadeh, A.; Toon, O. B. *Geophys. Res. Lett.* **1998**, *25*, 1379.
(48) Mozurkewich, M.; Calvert, J. G. *J. Geophys. Res.* **1988**, *93*, 15889.